Robust cosmic-ray constraints on p-wave annihilating MeV dark matter

Mathieu Boudaud, Thomas Lacroix, Martin Stref, Julien Lavalle

Robust cosmic-ray constraints on p-wave annihilating MeV dark matter

Mathieu Boudaud,[1,*] Thomas Lacroix,[2,†] Martin Stref,[2,‡] and Julien Lavalle[2,§]

[1] *Laboratoire de Physique Théorique et Hautes Énergies (LPTHE), UMR 7589 CNRS & UPMC, 4 Place Jussieu, F-75252 Paris – France*

[2] *Laboratoire Univers & Particules de Montpellier (LUPM), CNRS & Université de Montpellier (UMR-5299), Place Eugène Bataillon, F-34095 Montpellier Cedex 05 — France*

We recently proposed a method to constrain s-wave annihilating MeV dark matter from a combination of the Voyager 1 and the AMS-02 data on cosmic-ray electrons and positrons. Voyager 1 actually provides an unprecedented probe of dark matter annihilation to cosmic rays down to ~ 10 MeV, in an energy range where the signal is mostly immune to uncertainties in cosmic-ray propagation. In this letter, we derive for the first time new constraints on p-wave annihilation down to the MeV mass range using cosmic-ray data. To proceed, we derive a self-consistent velocity distribution for the dark matter across the Milky Way by means of the Eddington inversion technique and its extension to anisotropic systems. As inputs, we consider state-of-the-art Galactic mass models including baryons and constrained on recent kinematic data, allowing for both a cored or a cuspy halo. We then calculate the flux of cosmic-ray electrons and positrons induced by p-wave annihilating dark matter and obtain very stringent limits in the MeV mass range, robustly excluding cross sections greater than $\sim 10^{-22}\mathrm{cm}^3/\mathrm{s}$ (including theoretical uncertainties), about 5 orders of magnitude better than current CMB constraints. This limit assumes that dark matter annihilation is the sole source of cosmic rays, and could therefore be made even more stringent when reliable models of astrophysical backgrounds are included.

PACS numbers: 12.60.-i,95.35.+d,96.50.S-,98.35.Gi,98.70.Sa

Thermal dark matter (DM) is one of the most appealing DM scenario owing to its simplicity and to the fact that it can be experimentally or observationally tested. It predicts that DM is made of exotic particles with couplings to known elementary particles, such that they can be produced in the early universe and driven to thermal equilibrium before their comoving abundance is frozen as expansion takes over annihilation [1, 2]. If this decoupling occurs when DM is non-relativistic, we are left with cold DM (CDM), leading to a compelling cosmological structure formation scenario [3]. A prototypical candidate is the WIMP (weakly-interacting massive particle), which is currently actively searched for by a series of experiments. If the dark sector is not overly complex, the typical relevant mass range for DM particles exhibiting a thermal spectrum is $\sim$ 10 keV-100 TeV, which is bound from below by structure formation [4–8], and from above by unitarity limits [9]. The lower mass bound can be raised up to the MeV scale for WIMPs arising in minimal dark sectors [10], still leaving a wide range of possibilities [11]. The GeV-TeV scale is already under assault thanks to the direct and indirect detection techniques (for reviews, see *e.g.* [12–15]), and also thanks to particle colliders (*e.g.* [16, 17]). However, the sub-GeV and multi-TeV mass ranges are much less constrained and represent very interesting windows yet to be explored, with the former potentially leading to interesting cosmological signatures [10, 18]. In this letter, we will mostly focus on the sub-GeV scale.

The annihilation properties of WIMPs usually help define the most relevant search strategy. The annihilation rate, proportional to the average velocity-weighted annihilation cross section $\langle\sigma v\rangle$, is constrained at the time of chemical decoupling by the cosmological DM abundance [1, 19–21]. In the CDM scenario, WIMPs decouple when non-relativistic in the early universe at a temperature $T_\mathrm{f} = m_\chi/x_\mathrm{f}$, where m_χ is the WIMP mass and $x_\mathrm{f} \sim 20$. In most cases, the annihilation cross section can be expanded in powers of $x^{-1} \equiv (m_\chi/T)^{-1} \propto v^2 \ll 1$ (see some exceptions in [22]). Making the units explicit, we may write this expansion as

$$\begin{aligned}\langle\sigma v\rangle &= \langle\sigma v\rangle_{s\text{-wave}} + \langle\sigma v\rangle_{p\text{-wave}} + \text{higher orders} \quad (1)\\ &= \sigma_0\, c + \sigma_1\, c\, \langle\frac{v_\mathrm{r}^2}{c^2}\rangle + \mathcal{O}\left(\frac{v_\mathrm{r}^4}{c^4}\right),\end{aligned}$$

where σ_0 and σ_1 are model-dependent cross-section terms that encode the WIMP interaction properties, $v_\mathrm{r} \ll c$ is the relative WIMP speed (in a 2-particle system), c is the speed of light, and $\langle\rangle$ denotes an average over the velocity distribution.[1] This form is particularly well suited to con-

* boudaud@lpthe.jussieu.fr
† thomas.lacroix@umontpellier.fr
‡ martin.stref@umontpellier.fr
§ lavalle@in2p3.fr

[1] In the context of the relic density calculation where a Maxwell-Boltzmann distribution is assumed for WIMPs, the expansion is often made in terms of inverse powers of $x \equiv m_\chi/T$, T being the WIMP temperature. The correspondence with Eq. (1) is $\sigma_1\langle v_\mathrm{r}^2\rangle \leftrightarrow (3/2)\sigma_1/x$, here in natural units. For a computation in galactic halos, the speed v_r to average over is the *relative* speed between annihilating particles.

sistently compare the constraints coming from very different probes. The speed-independent term $\propto \sigma_0$ is called s-wave annihilation in analogy with the partial-wave expansion technique. WIMPs annihilating through s-wave terms can easily be probed by indirect searches because they efficiently annihilate in regions and/or epochs where DM is locally dense enough. This is for example the case at the time of recombination when the cosmic microwave background (CMB) was emitted, or in the centers of galactic halos in the present universe. The next annihilation term $\propto \sigma_1$ is called p-wave annihilation. In the following, we will concentrate on the latter and assume that $\sigma_0 = 0$.

The WIMP relic abundance sets constraints on the annihilation cross section at a speed – or inverse temperature – in the early universe ($v^2 \sim 3\,T/m_\chi \sim 0.15$), typically much larger than that in galactic halos ($v^2 \sim 10^{-6}$), and even much larger than at the recombination epoch ($v^2 \sim 10^{-9}$). This has no impact on the s-wave annihilation rate which only depends on the squared DM density, but makes p-wave annihilation much more difficult to probe with indirect searches. Instead, p-wave annihilating WIMPs can be more efficiently probed by direct searches, because rotated annihilation Feynmann diagrams correspond to elastic scattering which is usually not velocity-suppressed when annihilation is. A classical example is that of fermionic WIMPs annihilating into standard model fermions through a neutral scalar mediator in the s-channel [23]. However, direct DM searches are currently mostly efficient in the GeV-TeV mass range [24], leaving the sub-GeV mass range unexplored (but see [25, 26]).

We recently derived [27] strong constraints on s-wave annihilating MeV DM from measurements of MeV cosmic-ray (CR) electrons and positrons by the famous Voyager 1 (V1) spacecraft, launched in 1977 [28]. V1 crossed the heliopause in 2012, which has allowed it to collect interstellar sub-GeV CRs prevented by the solar magnetic field from reaching the Earth [29, 30]. Our bounds were extended to ∼TeV energies thanks to the AMS-02 data on positron CRs [31]. These limits are nicely complementary to those extracted from the CMB data [32–36], a completely different probe. In the present letter, we go beyond these results and compute the V1 and AMS-02 constraints on p-wave annihilation in detail. As we will see, in contrast to the s-wave case, these constraints will be much more stringent than those inferred from the CMB [35] or the diffuse extragalactic gamma-ray background (EGB) [37, 38].

In the p-wave annihilation rate, the cross section no longer factorizes out of the volume integral of the squared WIMP mass density ρ^2. Indeed, the cross section has an explicit relative-speed dependence which is itself expected to vary across the Galactic halo. Therefore, the source term for the injection of CR electrons and positrons becomes:

$$\mathcal{Q}^{p\text{-wave}}_{e^+/e^-}(\vec{x},E) = \delta_\chi \frac{\sigma_1\, c}{2}\left\{\frac{\rho(\vec{x})}{m_\chi}\right\}^2 \frac{dN_{e^+/e^-}}{dE} \times \int d^3\vec{v}_1 \int d^3\vec{v}_2\, \frac{|\vec{v}_2-\vec{v}_1|^2}{c^2} f_{\vec{v}}(\vec{v}_1,\vec{x})\, f_{\vec{v}}(\vec{v}_2,\vec{x}) = \delta_\chi \frac{\sigma_1\, c}{2}\frac{dN_{e^+/e^-}}{dE}\left\{\frac{\rho_{\rm eff}(\vec{x})}{m_\chi}\right\}^2 , \quad (2)$$

with

$$\rho^2_{\rm eff}(\vec{x}) \equiv \rho^2(\vec{x}) \int d^3\vec{v}_1 \int d^3\vec{v}_2 \frac{|\vec{v}_2-\vec{v}_1|^2}{c^2} f_{\vec{v}}(\vec{v}_1,\vec{x})\, f_{\vec{v}}(\vec{v}_2,\vec{x}) = \rho^2(\vec{x})\langle\frac{v_{\rm r}^2}{c^2}\rangle_{\vec{v}_1,\vec{v}_2}(\vec{x}) , \quad (3)$$

where $\delta_\chi = 1$ (1/2) for Majorana (Dirac) DM fermions, $dN_{e^+/e^-}/dE$ is the injected electron-positron spectrum, and $f_{\vec{v}}(\vec{v},\vec{x})$ is the normalized WIMP velocity distribution that depends on the position in the Milky Way (MW). For each annihilation final state, the injected CR spectrum will be determined from the Micromegas numerical package [39], based on the Pythia Monte Carlo generator [40]. All allowed final-state radiation processes are included.

Eq. (3) shows that an important input in the p-wave signal is the velocity distribution function (DF) of WIMPs in the system of interest. In many p-wave studies, the latter is often assumed to be a Maxwell-Boltzmann (MB) distribution, either with a constant velocity dispersion, or using the circular velocity as a proxy for the velocity dispersion. While the MB approximation is perfectly sound in the early universe up to CMB times, it is much more dubious in galaxies, which do not behave as isothermal spheres, especially in the densest central regions [41, 42]. In this work, we adopt a more theoretically motivated approach based on the Eddington inversion method [43], which relates the phase-space DF of WIMPs to their mass density profile and the total potential of the MW (including baryons) – see Ref. [44] for an extensive critical review, to which we refer the reader for all technical details (see also [45–47]). This approach allows us to describe isotropic as well as anisotropic systems [48–50], assuming spherical symmetry for the dark halo and the total gravitational potential. This actually provides a much better *predictive* description of hydrodynamical cosmological simulations than the MB approximation, even in the maximally symmetric approximation (spherical symmetry and isotropy), especially in the central regions of galactic halos [51].

To compute the phase-space DF of WIMPs from the Eddington inversion method, we use the Galactic mass model of Ref. [52], which is constrained against a series of recent kinematic data. It includes a spherical DM halo (scaling in radius r as $\propto r^{-\gamma}$ in the center, with $\gamma \in [0,1]$, and as $\propto r^{-3}$ at large radii), and baryonic components comprising a bulge and three disks (the thin and thick stellar disks, and a gaseous disk). All baryonic components are "sphericized" to compute the DM DF [44]. To account for uncertainties in the DM anisotropy,

we considered both isotropic and anisotropic DFs. In the latter case, we explore a wide range of possibilities by using both the radially anisotropic Osipkov-Merritt (OM) model with an anisotropy radius r_a set to the scale radius r_s of the DM halo profile, and a tangentially anisotropic model with a constant anisotropy parameter $\beta = -0.3$. To further account for uncertainties in the dark halo shape, we consider two inner-profile indices, $\gamma = 1/4$ (cored-like profile) and $\gamma = 1$ (cuspy profile à la Navarro-Frenk-White – NFW [53, 54]). Taking a fully cored profile would break necessary conditions for dynamical stability of the DF [44]. Disregarding stability of the DF and forcing $\gamma = 0$ would anyway provide results very similar to $\gamma = 0.25$, which is therefore a very conservative case.

Eq. (2) is the source term of a steady-state CR transport equation [55, 56], whose parameters (related to spatial diffusion, energy losses, reacceleration, and convection) are standardly calibrated on secondary-to-primary ratios [14, 57–63]. In the context of electron and positron CRs, we can solve this equation by means of the *pinching* semi-analytical method introduced in Ref. [64], compatible with the USINE framework [63]. This method capitalizes over previous analytical developments optimized for energies beyond the GeV [65–67], but improves on the low-energy part where radiative energy losses in the disk, diffusive reacceleration, and convection can dominate over spatial diffusion. It basically allows us to recast an equation where part of the energy losses occurs all over the magnetic halo by another analytically solvable equation where all losses are pinched into an infinitely thin disk (see also [68]) – this limit is justified as the Galactic disk half-height $h \sim 100$ pc is much smaller than that of the magnetic halo, $L \gtrsim 5$ kpc [64, 69, 70]. Both equations have solutions strictly equivalent *in the disk*, and the latter can hence be used in the context of local DM searches. In this work (and [71]), we slightly modify it to get more accurate results when the propagation length gets smaller than h, in which case the pinching approximation breaks down. In this regime, however, the spatial boundaries of the magnetic halo become irrelevant such that the infinite 3D solution [67, 68, 72] safely applies. This typically occurs at energies close to the injected energy. This correction is therefore important to accurately compute the local flux induced by a quasi-monochromatic injection, like in the process $\chi\bar{\chi} \to e^+e^-(\gamma)$. A non-singular transition is further easily implemented between the two regimes. The same approach is used to predict the secondary positron background induced by the scattering of CR nuclei off the interstellar medium (ISM), and provides better precision than previous similar calculations [64, 68, 72, 73]. While we expect additional primary contributions in the sub-GeV range from electron-positron sources like pulsars [72, 74–78], likely responsible for the rise in the positron fraction beyond a few GeV [79–81], we will not include them here because associated predictions are still plagued with large theoretical uncertainties. Therefore, our limits on DM annihilation can be considered as very conservative.

For CR propagation, we use two extreme cases identified in Ref. [27]: one with strong reacceleration (model A), allowing CR electrons and positrons to get energies higher than the WIMP mass in the MeV range; another with negligible reacceleration (model B). In both cases, energy losses in the MeV range have a timescale much smaller than the then subdominant spatial diffusion and convection processes (no longer true in the GeV range). Model A is the MAX model proposed in [59, 83], whose main feature beside a pseudo-Alfven velocity $V_a \sim 100$ km/s is a large magnetic halo with $L = 15$ kpc, making it a very optimistic setup for DM signal predictions. Though calibrated on old secondary-to-primary CR data, this setup is still valid for its general characteristics [84]. Model B is the model of Ref. [70] best-fitting the recent AMS-02 B/C data [85], and accounting for a spectral break in the diffusion coefficient [86–93]. It is very conservative because it assumes the smallest possible magnetic halo with $L = 4.1$ kpc [69, 70, 94] (hence minimizing the yield from DM annihilation), and has negligible reacceleration, reducing the flux predictions below a few GeV.

Since losses in the MeV range are caused by radiative interactions with the ISM, whose average properties over ~ 100-pc scales are well controlled [95, 96], uncertainties in the diffusion parameters have no impact on predictions in this energy range. Model B thus provides a robust and conservative limit as far as interstellar CR propagation is concerned [27]. Moreover, for predictions associated with the energy range covered by V1, solar modulation of CRs [97] is irrelevant and does not contribute additional uncertainties. In the AMS-02 range (∼GeV and above), we use the so-called force-field approximation [98, 99] to deal with solar modulation, with a conservative Fisk potential estimate of $\phi = 830$ MV [100]. In the GeV range, spatial diffusion takes over, and propagation uncertainties can in principle be larger. However, above a few tens of GeV, inverse Compton and synchrotron losses become the main transport processes and propagation uncertainties reduce to those in the magnetic and interstellar radiation fields (B-field [101, 102] and ISRF [103]) — in this high-energy limit, both propagation models converge, and solar modulation becomes irrelevant again. Uncertainties related to the DM density profile are estimated by considering both the cored-like and NFW profiles introduced above, whose fits to kinematic data provide a very similar local DM density $\rho_\odot \simeq 0.01\,M_\odot/\mathrm{pc}^3$ [52]. We also evaluate the impact of uncertainties in the velocity DF by considering both radially and tangentially anisotropic DFs, beside a reference isotropic DF.

We get limits on the p-wave cross section of Eq. (1) as a function of the WIMP mass assuming a full annihilation in $e^+e^-(\gamma)$. Our results are shown in Fig. 1, where the left (right) panel corresponds to the $\gamma = 0.25$ (1) halo profile. We also show complementary bounds obtained with the CMB [34, 35] (purple) rescaled to the latest Planck results [36], the high-redshift intergalac-

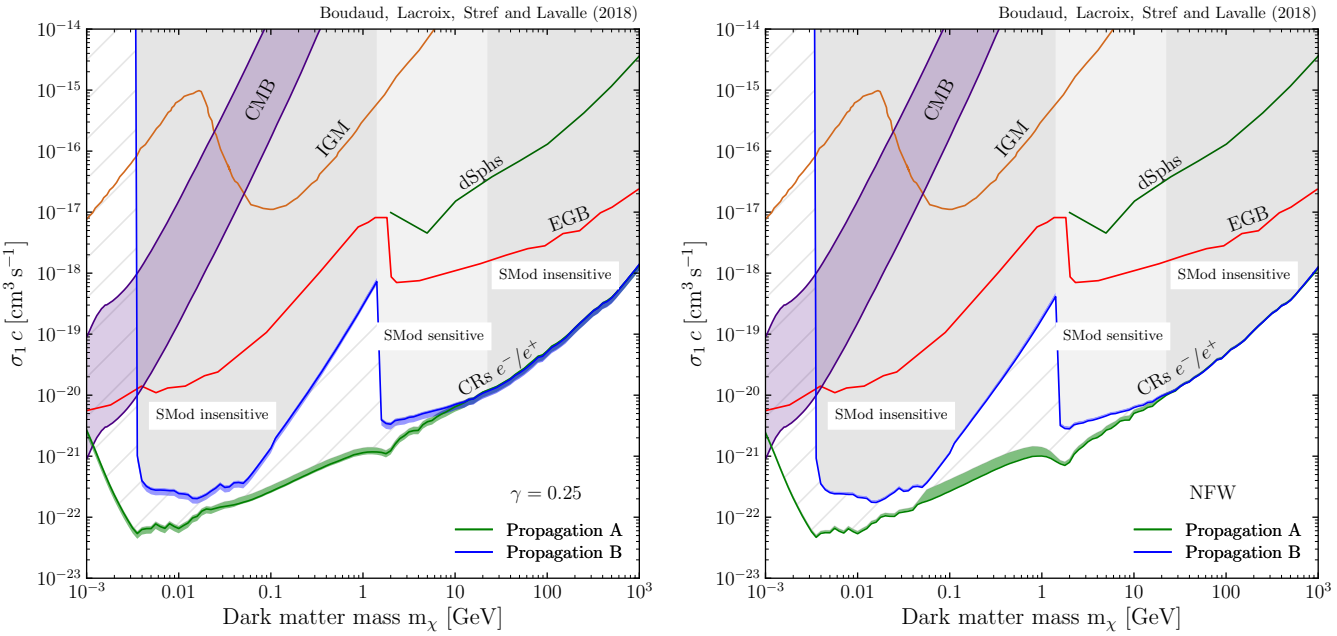

FIG. 1: Limits on the p-wave cross section as a function of the WIMP mass m_χ, in the 100% $\chi\bar{\chi} \to e^+e^-(\gamma)$ channel, for a high-reacceleration propagation model (model A – green curve) or a reacceleration-less, very conservative, propagation model (model B – blue curve). Uncertainty bands account for uncertainties in the anisotropy of the WIMP velocity DF. Also shown are the limits obtained with the CMB [34–36], IGM [35], EGB [37, 38], and gamma-ray observations of dwarf galaxies [82]. **Left panel**: cored-like DM density profile with $\gamma = 0.25$ [52]. **Right panel**: cuspy DM density profile with $\gamma = 1$ [52].

tic medium (IGM) temperature [35] (orange), the diffuse EGB [37, 38] (red), and gamma-ray observations of MW-satellite dwarf galaxies [82] (dark green curve). The CMB bound extrapolates the one obtained for s-wave annihilation by assuming a MB DF with a temperature at redshift ~ 600 that depends on the WIMP kinetic decoupling temperature $T_{\rm kd}$. We adopt two extreme values for the ratio $x_{\rm kd} = m_\chi/T_{\rm kd}$, 10^2 and 10^4, to cover most of the relevant parameter (the CMB limit is $\propto x_{\rm kd}^{-1}$).

Our limits are shown for both propagation models A (green) and B (blue curve), and the region for which solar modulation of CRs is irrelevant (relevant) is indicated as "SMod insensitive" ("SMod sensitive"). The associated shaded areas account for uncertainties induced by the unknown anisotropy of the WIMP DF. We emphasize that the limit obtained for model B is very conservative. Moreover, associated propagation uncertainties in the sub-GeV V1 region reduce to those in the low-energy energy losses, which are very small. This conservative result is strikingly more constraining than complementary searches, by more than two orders of magnitude in the 5-100 MeV mass range, making CRs remarkable probes of p-wave annihilation. This contrasts with constraints obtained on s-wave annihilation, for which CMB bounds are stronger. Indeed, as velocity factors enter the annihilation rate, the CMB probe is penalized by a DM temperature much lower at the recombination epoch than in virialized galactic halos today. Moreover, the CR probe has the advantage over gamma-ray observations that predictions saturate the data with very small annihilation cross sections without considering any background. The secondary background is in effect completely negligible in the V1 energy range [27], while it gets close to the low-energy AMS-02 positron data though in a regime where solar modulation matters.

We note that our strongly improved limit lies now only at two orders of magnitude from the p-wave cross section required for the correct WIMP abundance, $\sim 10^{-24}$cm^3/s. Moreover, we stress that it already excludes some interesting WIMP models with enriched dark sectors, *e.g.* that of Ref. [104]. Our work thus provides stringent constraints on particle model building along this line.

To summarize, we have used the electron and positron data from V1 and the positron data from AMS-02 to constrain p-wave annihilating DM. We have obtained limits that are much more stringent than those derived from complementary astrophysical messengers in the MeV-TeV energy range. Those derived for our very conservative model B are very robust in the V1 range (below the GeV), because the flux predictions then only depend on the average ISM properties, on the halo model, and on the anisotropy level in the DM DF. We have shown in Fig. 1 that using a kinematically constrained cored vs. cuspy halo does not alter our result, nor does spanning different anisotropy configurations. Moreover, above few tens of GeV, solar modulation gets irrelevant again, and CR propagation is then set by inverse-Compton and syn-

chrotron losses, for which uncertainties reduce to those in the local ISRF and B-field. We emphasize that these limits could be made even more severe if additional astrophysical primary contributions were considered [105]. This will likely be done in the future when more detailed low-energy CR studies succeed in more reliably modeling the yield from these astrophysical sources.

ACKNOWLEDGMENTS

We wish to thank Pierre Salati for early participation in this project. We also thank Alan C. Cummings and Martin Winkler for valuable exchanges. MB acknowledges support from the European Research Council (ERC) under the EU Seventh Framework Program (FP7/2007-2013)/ERC Starting Grant (agreement n. 278234 — NewDark project led by M. Cirelli). TL, JL, and MS are partly supported by the OCEVU Labex (ANR-11-LABX-0060), the IN2P3-theory/PNHE/PNCG project "Galactic Dark Matter", and European Union's Horizon 2020 research and innovation program under the Marie Skłodowska-Curie grant agreements No 690575 and No 674896 – in addition to recurrent funding by CNRS and the University of Montpellier.

Appendix A: Effective density profile

In this section, we show the detailed results obtained for the effective squared density profile defined in Eq. (3). They are displayed on Fig. 2. The original squared profile are shown in blue ($\gamma = 0.25$) and red ($\gamma = 1$) crosses (rescaled by a factor of $\sim 10^{-6} \sim (\sigma_v/c)^2$, where σ_v is the velocity dispersion in the Milky Way), while the velocity-corrected profiles are shown in solid (dashed, dot-dashed, and dotted) curves for the isotropic (constant tangential anisotropy, spatial-dependent radial anisotropy, and Maxwellian) velocity DF. The bottom part of the plot shows the residuals with respect to the isotropic, reference case. For the Maxwellian calculation, the velocity dispersion is taken proportional to the circular velocity, consistently with the isothermal sphere approximation [42]. We see that the velocity-weighted squared profiles lead to suppressed annihilation luminosity with respect to the standard case. We also see that the Maxwell-Boltzmann approximation strongly undershoots the luminosity arising from the other predictions, which turn out to be much better supported both by theory and simulations [44, 51]. We have discarded the unrealistic Maxwellian case from our limits.

Note that when going to CR flux predictions, diffusion plays the role of averaging the luminosity over the CR horizon which is set by the dominant transport process at a given energy. Therefore, to figure out the local CR yield induced by DM p-wave annihilation, one needs to average the effective luminosity over the relevant volume around the observer, who sits at $r \sim 8$ kpc from the Galactic center.

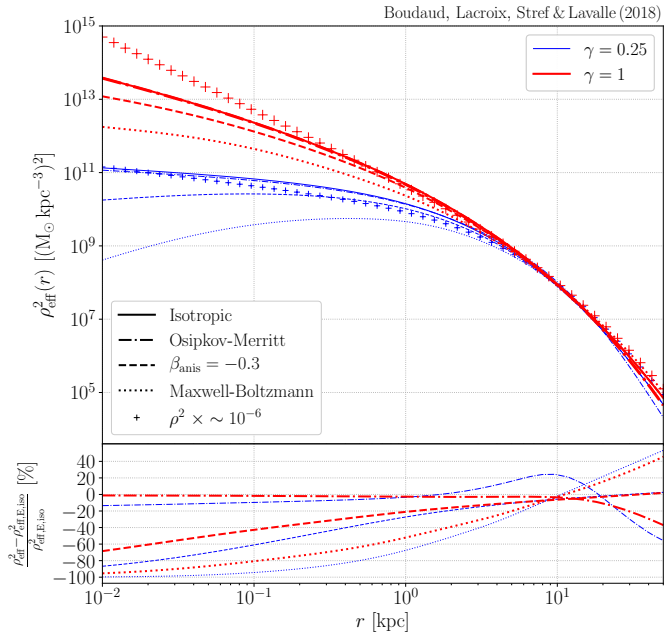

FIG. 2: Effective squared density profiles, which translate the impact of the spatial-dependent average squared relative velocity. The effective profiles are shown for different assumptions for the WIMP velocity DF, made explicit in the legend.

Appendix B: Bounds on various annihilation channels

In Fig. 3, we show the conservative limits we get for different annihilation final states (propagation model B, and cored-like halo profile with $\gamma = 0.25$). We see that for final-state particle masses above a few GeV, limits are dominated by the AMS-02 data. In contrast, the Voyager data are very powerful in constraining leptonic channels.

Appendix C: Detailed view on theoretical uncertainties

In this section, we provide additional details about the origin of the uncertainties that were featured as shaded areas around the limits shown in Fig. 1. They originate from the different assumptions made for the anisotropy in the velocity DF, which is not firmly predicted by the non-linear theory and could therefore vary from a galaxy to another. In order to span the most likely configurations, we adopted two contrasting cases, one with constant tangential anisoptropy, another with spatial-dependent radial (OM) anisotropy, on top on the isotropic Eddington case and the simplistic Maxwellian approximation. The limits obtained for these different configurations are

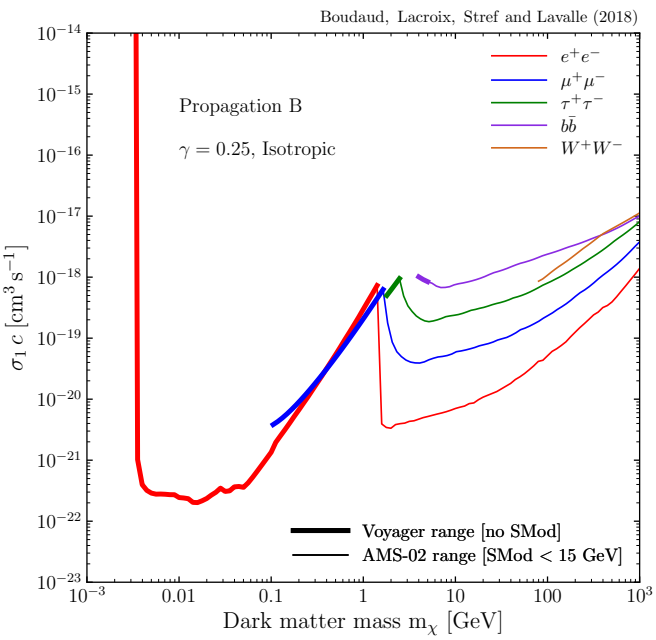

FIG. 3: Limits on the p-wave annihilation cross section obtained for different annihilation channels, using the most conservative setup for the CR flux predictions: propagation model B (no reacceleration, minimal magnetic halo size ~ 4 kpc), and a cored-like halo profile ($\gamma = 0.25$).

shown in Fig. 4. The top (bottom) panels correspond to the cored-like (NFW) halo with $\gamma = 0.25$ ($\gamma = 1$). The left (right) panels are associated with CR predictions made with optimistic (very conservative) propagation model A (B) that is characterized by a strong reacceleration and $L = 15$ kpc (no reacceleration and $L = 4.1$ kpc). All panels display the limits obtained for all the velocity DFs mentioned above. These results can be easily interpreted from the hierarchy in the luminosity yield shown in Fig. 2.

[1] B. W. Lee and S. Weinberg, Phys. Rev. Lett. **39**, 165 (1977).
[2] J. R. Bond, A. S. Szalay, and M. S. Turner, Phys. Rev. Lett. **48**, 1636 (1982).
[3] P. J. E. Peebles, Astrophys. J. Lett. **263**, L1 (1982).
[4] S. Colombi, S. Dodelson, and L. M. Widrow, Astrophys. J. **458**, 1 (1996), astro-ph/9505029.
[5] M. Viel, J. Lesgourgues, M. G. Haehnelt, S. Matarrese, and A. Riotto, Phys. Rev. D **71**, 063534 (2005), astro-ph/0501562.
[6] M. Viel, G. D. Becker, J. S. Bolton, and M. G. Haehnelt, Phys. Rev. D **88**, 043502 (2013), arXiv:1306.2314 [astro-ph.CO].
[7] S. Bose, W. A. Hellwing, C. S. Frenk, A. Jenkins, M. R. Lovell, J. C. Helly, and B. Li, MNRAS **455**, 318 (2016), arXiv:1507.01998.
[8] J. Baur, N. Palanque-Delabrouille, C. Yèche, A. Boyarsky, O. Ruchayskiy, É. Armengaud, and J. Lesgourgues, JCAP **12**, 013 (2017), arXiv:1706.03118.
[9] K. Griest and M. Kamionkowski, Phys. Rev. Lett. **64**, 615 (1990).
[10] R. J. Wilkinson, J. Lesgourgues, and C. Bœhm, JCAP **4**, 026 (2014), arXiv:1309.7588.
[11] R. K. Leane, T. R. Slatyer, J. F. Beacom, and K. C. Y. Ng, Phys. Rev. D **98**, 023016 (2018), arXiv:1805.10305 [hep-ph].
[12] J. D. Lewin and P. F. Smith, Astroparticle Physics **6**, 87 (1996).
[13] K. Freese, M. Lisanti, and C. Savage, Reviews of Modern Physics **85**, 1561 (2013), arXiv:1209.3339.
[14] J. Lavalle and P. Salati, Comptes Rendus Physique **13**, 740 (2012), arXiv:1205.1004 [astro-ph.HE].
[15] T. Bringmann and C. Weniger, Physics of the Dark Universe **1**, 194 (2012), arXiv:1208.5481 [hep-ph].
[16] M. Fairbairn, A. C. Kraan, D. A. Milstead, T. Sjöstrand, P. Skands, and T. Sloan, Phys. Rept. **438**, 1 (2007), hep-ph/0611040.
[17] F. Kahlhoefer, International Journal of Modern Physics A **32**, 1730006 (2017), arXiv:1702.02430 [hep-ph].
[18] L. Lopez-Honorez, O. Mena, Á. Moliné, S. Palomares-Ruiz, and A. C. Vincent, JCAP **8**, 004 (2016), arXiv:1603.06795.
[19] P. Binétruy, G. Girardi, and P. Salati, Nuclear Physics B **237**, 285 (1984).
[20] M. Srednicki, R. Watkins, and K. A. Olive, Nuclear Physics B **310**, 693 (1988).
[21] P. Gondolo and G. Gelmini, Nuclear Physics B **360**, 145 (1991).
[22] K. Griest and D. Seckel, Phys. Rev. D **43**, 3191 (1991).
[23] J. Abdallah, *et al.*, Physics of the Dark Universe **9**, 8 (2015), arXiv:1506.03116 [hep-ph].
[24] T. Marrodán Undagoitia and L. Rauch, Journal of Physics G Nuclear Physics **43**, 013001 (2016), arXiv:1509.08767 [physics.ins-det].
[25] R. Essig, J. Mardon, and T. Volansky, Phys. Rev. D **85**, 076007 (2012), arXiv:1108.5383 [hep-ph].
[26] C. Kouvaris and J. Pradler, Phys. Rev. Lett. **118**, 031803 (2017), arXiv:1607.01789 [hep-ph].
[27] M. Boudaud, J. Lavalle, and P. Salati, Phys. Rev. Lett. **119**, 021103 (2017), arXiv:1612.07698 [astro-ph.HE].

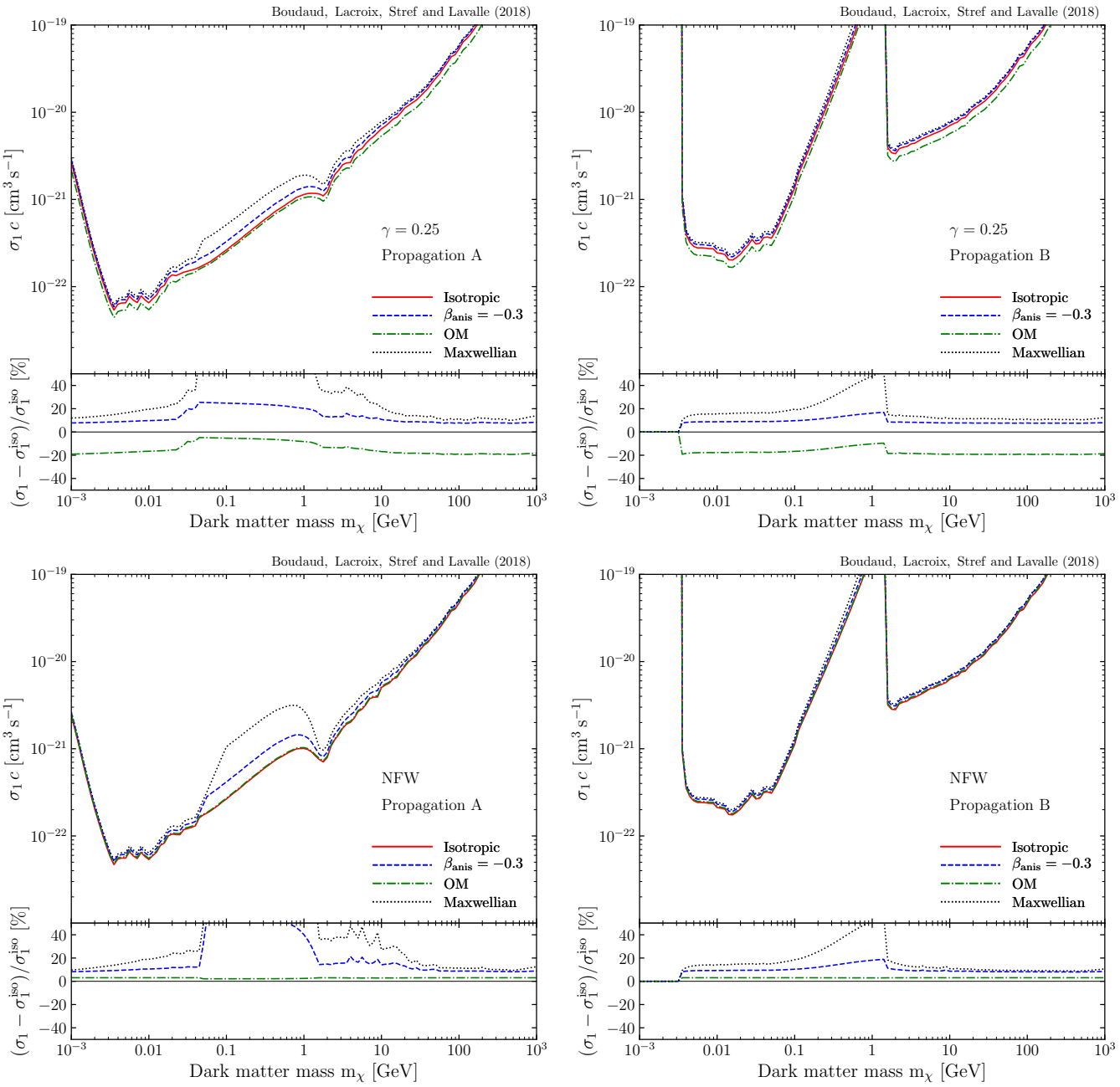

FIG. 4: Impact of different assumptions for the anisotropy in the velocity DF, and relative comparison to the Eddington-inverted isotropic DF (solid red curves). The black dotted curves show the results obtained for the Maxwellian approximation, the blue dashed curves correspond to a constant anisotropy parameter $\beta = -0.3$ (tangential anisotropy), and the green dash-dotted curves correspond to the Osipkov-Merrit model with an anisotropy radius set to the scale radius of the DM halo. **Left (right) panels**: propagation model A (B). **Top (bottom) panels**: cored (NFW) DM halo.

[28] S. M. Krimigis, C. O. Bostrom, T. P. Armstrong, W. I. Axford, C. Y. Fan, G. Gloeckler, and L. J. Lanzerotti, Space Science Rev. **21**, 329 (1977).

[29] E. C. Stone, A. C. Cummings, F. B. McDonald, B. C. Heikkila, N. Lal, and W. R. Webber, Science **341**, 150 (2013).

[30] A. C. Cummings, E. C. Stone, B. C. Heikkila, N. Lal, W. R. Webber, G. Jóhannesson, I. V. Moskalenko, E. Orlando, and T. A. Porter, Astrophys. J. **831**, 18 (2016).

[31] AMS-02 Collaboration, M. Aguilar, *et al.*, Phys. Rev. Lett. **113**, 121102 (2014).

[32] J. A. Adams, S. Sarkar, and D. W. Sciama, MNRAS **301**, 210 (1998), astro-ph/9805108.

[33] X. Chen and M. Kamionkowski, Phys. Rev. D **70**, 043502 (2004), astro-ph/0310473.

[34] T. R. Slatyer, Phys. Rev. D **93**, 023527 (2016), arXiv:1506.03811 [hep-ph].
[35] H. Liu, T. R. Slatyer, and J. Zavala, Phys. Rev. D **94**, 063507 (2016), arXiv:1604.02457.
[36] Planck Collaboration, Y. Akrami, *et al.*, ArXiv e-prints (2018), arXiv:1807.06205.
[37] R. Essig, E. Kuflik, S. D. McDermott, T. Volansky, and K. M. Zurek, Journal of High Energy Physics **11**, 193 (2013), arXiv:1309.4091 [hep-ph].
[38] A. Massari, E. Izaguirre, R. Essig, A. Albert, E. Bloom, and G. A. Gómez-Vargas, Phys. Rev. D **91**, 083539 (2015), arXiv:1503.07169 [hep-ph].
[39] G. Bélanger, F. Boudjema, A. Goudelis, A. Pukhov, and B. Zaldívar, Computer Physics Communications **231**, 173 (2018), arXiv:1801.03509 [hep-ph].
[40] T. Sjöstrand, S. Ask, J. R. Christiansen, R. Corke, N. Desai, P. Ilten, S. Mrenna, S. Prestel, C. O. Rasmussen, and P. Z. Skands, Computer Physics Communications **191**, 159 (2015), arXiv:1410.3012 [hep-ph].
[41] H. Mo, F. C. van den Bosch, and S. White, *Galaxy Formation and Evolution* (Cambridge University Press, 2010).
[42] J. Binney and S. Tremaine, *Galactic Dynamics*, 2nd ed., Princeton series in astrophysics (Princeton University Press, Princeton, NJ USA, 2008., 2008).
[43] A. S. Eddington, MNRAS **76**, 572 (1916).
[44] T. Lacroix, M. Stref, and J. Lavalle, JCAP **09**, 040 (2018), arXiv:1805.02403.
[45] F. Ferrer and D. R. Hunter, JCAP **9**, 005 (2013), arXiv:1306.6586 [astro-ph.HE].
[46] D. R. Hunter, JCAP **2**, 023 (2014), arXiv:1311.0256 [astro-ph.CO].
[47] K. K. Boddy, J. Kumar, and L. E. Strigari, Phys. Rev. D **98**, 063012 (2018), arXiv:1805.08379 [astro-ph.HE].
[48] L. P. Osipkov, Soviet Astronomy Letters **5**, 42 (1979).
[49] D. Merritt, Astron. J. **90**, 1027 (1985).
[50] P. Cuddeford, MNRAS **253**, 414 (1991).
[51] T. Lacroix, A. Nunez, M. Stref, J. Lavalle, and E. Nezri, In preparation (2018).
[52] P. J. McMillan, MNRAS **465**, 76 (2017), arXiv:1608.00971.
[53] J. F. Navarro, C. S. Frenk, and S. D. M. White, Astrophys. J. **462**, 563 (1996), astro-ph/9508025.
[54] H. Zhao, MNRAS **278**, 488 (1996), astro-ph/9509122.
[55] V. L. Ginzburg and S. I. Syrovatskii, *The Origin of Cosmic Rays* (New York: Macmillan, 1964).
[56] V. S. Berezinskii, S. V. Bulanov, V. A. Dogiel, and V. S. Ptuskin, *Astrophysics of cosmic rays* (North Holland, 1990).
[57] A. W. Strong and I. V. Moskalenko, Astrophys. J. **509**, 212 (1998), astro-ph/9807150.
[58] F. C. Jones, A. Lukasiak, V. Ptuskin, and W. Webber, Astrophys. J. **547**, 264 (2001), astro-ph/0007293.
[59] D. Maurin, F. Donato, R. Taillet, and P. Salati, Astrophys. J. **555**, 585 (2001), astro-ph/0101231.
[60] A. W. Strong, I. V. Moskalenko, and V. S. Ptuskin, Annual Review of Nuclear and Particle Science **57**, 285 (2007), astro-ph/0701517.
[61] R. Kissmann, Astroparticle Physics **55**, 37 (2014), arXiv:1401.4035 [astro-ph.HE].
[62] C. Evoli, D. Gaggero, A. Vittino, G. Di Bernardo, M. Di Mauro, A. Ligorini, P. Ullio, and D. Grasso, JCAP **2**, 015 (2017), arXiv:1607.07886 [astro-ph.HE].
[63] D. Maurin, ArXiv e-prints (2018), arXiv:1807.02968 [astro-ph.IM].
[64] M. Boudaud, E. F. Bueno, S. Caroff, Y. Genolini, V. Poulin, V. Poireau, A. Putze, S. Rosier, P. Salati, and M. Vecchi, Astron. Astroph. **605**, A17 (2017), arXiv:1612.03924 [astro-ph.HE].
[65] S. V. Bulanov and V. A. Dogel, Astrophys. Space Sci. **29**, 305 (1974).
[66] E. A. Baltz and J. Edsjö, Phys. Rev. D **59**, 023511 (1998), astro-ph/9808243.
[67] J. Lavalle, J. Pochon, P. Salati, and R. Taillet, Astron. Astroph. **462**, 827 (2007), arXiv:astro-ph/0603796.
[68] T. Delahaye, R. Lineros, F. Donato, N. Fornengo, J. Lavalle, P. Salati, and R. Taillet, Astron. Astroph. **501**, 821 (2009), arXiv:0809.5268.
[69] J. Lavalle, D. Maurin, and A. Putze, Phys. Rev. D **90**, 081301 (2014), arXiv:1407.2540 [astro-ph.HE].
[70] A. Reinert and M. W. Winkler, JCAP **1**, 055 (2018), arXiv:1712.00002 [astro-ph.HE].
[71] M. Boudaud and M. Cirelli, ArXiv e-prints (2018), arXiv:1807.03075 [astro-ph.HE].
[72] T. Delahaye, J. Lavalle, R. Lineros, F. Donato, and N. Fornengo, Astron. Astroph. **524**, A51 (2010), arXiv:1002.1910 [astro-ph.HE].
[73] J. Lavalle, MNRAS **414**, 985L (2011), arXiv:1011.3063 [astro-ph.HE].
[74] C. S. Shen, Astrophys. J. Lett. **162**, L181+ (1970).
[75] F. A. Aharonian, A. M. Atoyan, and H. J. Voelk, Astron. Astroph. **294**, L41 (1995).
[76] D. Hooper, P. Blasi, and P. Dario Serpico, JCAP **1**, 025 (2009), arXiv:0810.1527.
[77] S. Profumo, Central Eur.J.Phys. **10**, 1 (2011), arXiv:0812.4457.
[78] M. Boudaud, S. Aupetit, S. Caroff, A. Putze, G. Belanger, Y. Genolini, C. Goy, V. Poireau, V. Poulin, S. Rosier, P. Salati, L. Tao, and M. Vecchi, Astron. Astroph. **575**, A67 (2015), arXiv:1410.3799 [astro-ph.HE].
[79] HEAT Collaboration, M. A. DuVernois, *et al.*, Astrophys. J. **559**, 296 (2001).
[80] PAMELA Collaboration, O. Adriani,*et al.*, Nature **458**, 607 (2009), arXiv:0810.4995.
[81] AMS-02 Collaboration, M. Aguilar, *et al.*, Phys. Rev. Lett. **110**, 141102 (2013).
[82] Y. Zhao, X.-J. Bi, H.-Y. Jia, P.-F. Yin, and F.-R. Zhu, Phys. Rev. D **93**, 083513 (2016), arXiv:1601.02181 [astro-ph.HE].
[83] F. Donato, N. Fornengo, D. Maurin, P. Salati, and R. Taillet, Phys. Rev. D **69**, 063501 (2004), astro-ph/0306207.
[84] M. Boudaud, S. Caroff, Y. Génolini, V. Poulin, P.-I. Silva Batista, L. Derome, J. Lavalle, D. Maurin, V. Poireau, S. Rosier, P. Salati, P. D. Serpico, and M. Vecchi, In preparation (2018).
[85] AMS-02 Collaboration, M. Aguilar, *et al.*, Phys. Rev. Lett. **117**, 231102 (2016).
[86] CREAM Collaboration, H. S. Ahn, *et al.*, Astrophys. J. Lett. **714**, L89 (2010), arXiv:1004.1123 [astro-ph.HE].
[87] PAMELA Collaboration, O. Adriani, *et al.*, Science **332**, 69 (2011), arXiv:1103.4055 [astro-ph.HE].
[88] AMS-02 Collaboration, M. Aguilar, *et al.*, Phys. Rev. Lett. **114**, 171103 (2015).

[89] AMS-02 Collaboration, M. Aguilar, *et al.*, Phys. Rev. Lett. **115**, 211101 (2015).

[90] P. Blasi, E. Amato, and P. D. Serpico, Phys. Rev. Lett. **109**, 061101 (2012), arXiv:1207.3706 [astro-ph.HE].

[91] P. Blasi, MNRAS **471**, 1662 (2017), arXiv:1707.00525 [astro-ph.HE].

[92] Y. Génolini, P. D. Serpico, M. Boudaud, S. Caroff, V. Poulin, L. Derome, J. Lavalle, D. Maurin, V. Poireau, S. Rosier, P. Salati, and M. Vecchi, Phys. Rev. Lett. **119**, 241101 (2017), arXiv:1706.09812 [astro-ph.HE].

[93] C. Evoli, P. Blasi, G. Morlino, and R. Aloisio, Phys. Rev. Lett. **121**, 021102 (2018), arXiv:1806.04153 [astro-ph.HE].

[94] M. Boudaud, M. Cirelli, G. Giesen, and P. Salati, JCAP **5**, 013 (2015), arXiv:1412.5696 [astro-ph.HE].

[95] K. M. Ferrière, Reviews of Modern Physics **73**, 1031 (2001), astro-ph/0106359.

[96] G. Jóhannesson, T. A. Porter, and I. V. Moskalenko, Astrophys. J. **856**, 45 (2018), arXiv:1802.08646 [astro-ph.HE].

[97] M. Potgieter, Living Reviews in Solar Physics **10**, 3 (2013), arXiv:1306.4421 [physics.space-ph].

[98] L. J. Gleeson and W. I. Axford, Astrophys. J. **154**, 1011 (1968).

[99] L. A. Fisk, J. Geophys. Res. **76**, 221 (1971).

[100] A. Ghelfi, F. Barao, L. Derome, and D. Maurin, Astron. Astroph. **591**, A94 (2016), arXiv:1511.08650 [astro-ph.HE].

[101] X.-H. Sun and W. Reich, Research in Astronomy and Astrophysics **10**, 1287 (2010), arXiv:1010.4394.

[102] R. Jansson and G. R. Farrar, Astrophys. J. Lett. **761**, L11 (2012), arXiv:1210.7820 [astro-ph.GA].

[103] T. A. Porter, G. Jóhannesson, and I. V. Moskalenko, Astrophys. J. **846**, 67 (2017), arXiv:1708.00816 [astro-ph.HE].

[104] J. Choquette, J. M. Cline, and J. M. Cornell, Phys. Rev. D **94**, 015018 (2016), arXiv:1604.01039 [hep-ph].

[105] M. J. Boschini, S. Della Torre, M. Gervasi, D. Grandi, G. Jóhannesson, G. La Vacca, N. Masi, I. V. Moskalenko, S. Pensotti, T. A. Porter, L. Quadrani, P. G. Rancoita, D. Rozza, and M. Tacconi, Astrophys. J. **854**, 94 (2018), arXiv:1801.04059 [astro-ph.HE].